PROCEEDINGS OF SPIE

SPIEDigitalLibrary.org/conference-proceedings-of-spie

Lymph node micrometastases detection using paired-agent imaging protocol with biological tissue model

Li, Chengyue, Torres, Veronica, He, Yusheng, Xu, Xiaochun, Brankov, Jovan, et al.

Chengyue Li, Veronica C. Torres, Yusheng He, Xiaochun Xu, Jovan G. Brankov, Kenneth M. Tichauer, "Lymph node micrometastases detection using paired-agent imaging protocol with biological tissue model," Proc. SPIE 11243, Imaging, Manipulation, and Analysis of Biomolecules, Cells, and Tissues XVIII, 112431P (17 February 2020); doi: 10.1117/12.2546427



Event: SPIE BiOS, 2020, San Francisco, California, United States

Lymph node micrometastases detection using paired-agent imaging protocol with biological tissue model

Chengyue Li¹, Veronica C. Torres¹, Yusheng He¹, Xiaochun Xu², Jovan G. Brankov³, Kenneth M. Tichauer¹

ABSTRACT

Sentinel lymph node involvement is recognized as a prognostic factor in breast cancer staging and is essential to guide optimal treatment. The possibility of missed micrometastases by using conventional methods was estimated around 20-60% cases has created a demand for the development of more accurate approaches. A paired-agent imaging approach is presented by employing a control imaging agent to allow rapid, quantitative mapping of microscopic populations of tumor cells in lymph nodes to guide pathology sectioning. To test the feasibility of this approach to identify micrometastases, lymph node micrometastases biological tissue model was developed and were stained with targeted and control imaging agent solution to evaluate the binding potential of the agents of intact nodes. ABY-029, an EGFR specific affibody was labeled with IRDye-800CW(LICOR) as targeted agent and IRDye-700DX was hydrolyzed as control agent. Lymph nodes phantoms were stained for 60 min, followed by 60 min rinsing, and the fluorescence of whole lymph node phantoms were recorded to evaluate the spatial distribution of both agents in the entire phantom. Measured binding potential of targeted agent between micrometastases and control regions were 0.652 ± 0.130 and -0.008 ± 0.042 respectively (p < 0.0001). The results demonstrate the potential to enhance the sensitivity of lymph node pathology using paired-agent imaging in a whole human lymph node.

Keywords: paired-agent fluorescent imaging, micrometastses, lymph node

1. INTRODUCTION

The identification of cancer spread to tumor-draining lymph node is a key prognostic factor for staging and guiding adjuvant treatment in many cancer types, including breast, melanoma, head and neck, lung and gynecologic cancer[1], as the lymphatic system served as a primary route for metastasis[2]. Currently, lymph node dissection is considered as a standard care of cancer treatment and followed by pathology examination to evaluate lymph node tumor burden[3]. However, the conventional pathology laboratories only section lymph node as 5-µm-thick slices at 2-mm intervals, resulting less than 1% of lymph node volume was examinated. Hematoxylin and Eosin (H&E) staining was then performed which provides morphological information for pathologists to identify abnormal cells. It has been demonstrated that early stage metastasis disease might not be able to be detected by this routine sectioning procedure, as this method was aimed to detect tumor cells deposits greater than 2 mm in diameter, defined as macrometastases[4-6]. The estimation of undetected micrometastases using conventional method range from 20-60%[7], of which the probability increase with decreasing size of tumor.

Numerous studies have demonstrated that micrometastases have important prognostic implication and thus more sensitive methods of detecting cancer spread to lymph node could enable earlier intervention for guiding therapeutic

Imaging, Manipulation, and Analysis of Biomolecules, Cells, and Tissues XVIII, edited by Daniel L. Farkas, Attila Tarnok, Proc. of SPIE Vol. 11243, 112431P ⋅ © 2020 SPIE ⋅ CCC code: 1605-7422/20/\$21 ⋅ doi: 10.1117/12.2546427

¹Department of Biomedical Engineering, Illinois Institute of Technology, Chicago, IL 60616

²Department of Surgery-Research, Dartmouth-Hitchcock Medical Center, Lebanon, NH 03756

³Department of Electrical and Computer Engineering, Illinois Institute of Technology, Chicago, IL 60616

decision-making[8-10]. Many investigators have shown the improved micrometastases detection in lymph node by taking extensive serial sectioning and immunohistochemistry[11-13]. However, these approaches are not cost-effective and too labor-intensive to be practical. Yet, most of the methods still rely on sampling only a small fraction of the lymph node volume or involve digestion of the tissue such that subsequent pathology and direct assessment is impossible. Therefore, earlier and more accurate diagnostics of aggressive disease without requiring redundant time and resources is needed.

Motivated by the limitations of conventional histology approach, we developed a paired-agent imaging approach with a control imaging agent to allow rapid, quantitative mapping of microscopic populations of tumor cells in lymph nodes to guide pathology sectioning to reduce the false negative rate. Recently in a metastatic mouse model demonstrated that fewer than 200 cancer-cells can be accurately detected using a wide-field non-invasive imaging of human breast cancer spread to axillary lymph nodes[14]. While paired-agent imaging methodology can provide true molecular contrast between cancerous and healthy tissue, a low-cost fluorescence optical projection tomography (OPT) protocol was recently demonstrated for rapid imaging of whole lymph nodes in three dimensions[15]. By employing angular restriction of photon detection, a 3D mapping of cancer biomarkers in excised lymph nodes will be provided and guide pathologists to suspicious volumes. It was demonstrated through porcine lymph node metastases models the feasibility to detect and localize 200-µm-diameter metastases in 1-cm-diameter lymph nodes[16].

This proceeding was to demonstrate the ability of lymph node micrometastases detection with biological tissue model to evaluate the staining and rinsing protocol for further investigate the potential of paired-agent fluorescence imaging to detect micrometastases in resected lymph nodes.

2. METHODS AND RESULTS

2.1 Paired-agent kinetic model

The paired-agent molecular imaging estimate of targeted biomolecule concentration ("Binding Potential")[17] by employing a control imaging-agent that can essentially provides a means of correcting for the influence of tissue perfusion and non-specific uptake and retention on targeted imaging agent concentrations[18-21]. This approach assumes that the signal from the targeted imaging agent arises from concentration of imaging agent that is either bound to the specific receptor (C_b) or freely associated in the tissue (C_f) . By making the assumption that the control imaging agent signal approximates the free concentration of the targeted imaging agent, the following expression can be derived:

$$\frac{Targeted-Control}{Control} \cong \frac{C_f + C_b - C_f}{C_f} = \frac{C_b}{C_f} = K_A B \equiv Binding \ Potential \ \ (BP) \ ,$$

where K_A is the affinity of the targeted imaging agent (a constant under most conditions) and B represents the concentration of targeted biomolecules, which for cancer-specific molecules is proportional to the number cancer cells

For the ratiometric paired-agent imaging method to accurately estimate the binding potential or concentration of cancer cells in lymph node staining applications, both the targeted and control agents must diffuse equally to all regions of the node when the node is immersed in the solution of targeted imaging agent(s) and control imaging agent mixture in the absence of cancer cells in lymph nodes. This allows elucidation of specific binding effects from all nonspecific physiological effects on the delivery and retention of the targeted imaging agent in order to increase the sensitivity of cancer assessment.

2.2 Lymph node micrometastases biological tissue model

In order to mimic the clinical condition of cancer spread tumor draining lymph node, lymph node micrometastases biological tissue model was developed to evaluate the feasibility of the paired-agent imaging method to estimate the binding potential of cancer cells in resected lymph node. In comparison with most traditional 2D cell culture systems, 3D spheroids are more favorable for modeling caner and tissue biology as they represent a unique model to more accurately recapitulate micro-environment and cell-cell interaction, and also maintain their viability. [22-26]. Moreover, tumor spheroids would allow cancer cells express in its original 3D architecture and offers a better control of the size of metastases in lymph nodes. In the interest of developing micrometastases model in excised lymph nodes, breast cancer cells MDA-MB-231 tumor spheroids will be formed by suspending cells in culture medium containing 0.24% (w/v) methyl cellulose in round-bottom, low binding, 96-well plated and incubated over night at 37 °C and 5% CO₂. 1 ×10⁴ cells were seeded in each well to achieve spheroid size of 250 μm in diameter. Tumor spheroids formation was confirmed under bright field microscope.

Spheroids were collected into a 1.5mL microcentrifuge tube and allow spheroids to settle at the bottom of the microcentrifuge tube. Supernatant will be removed and then spheroids were resuspended in PBS solution. Lymph node mimicking phantom was develop using agarose gel to model biological tissue to evaluate staining and rinsing diffusion using paired-agent in this study. Agarose was combined with saline (3% w/v agarose/saline) and stir until agarose was suspended in translucent form. The solution was heated in a microwave and stir periodically until the mixture was brought to light boil. The mixture solution was then heated in 30 seconds intervals and repeatedly stirred until the solution turned entirely transparent and homogenous. The solution was placed on a magnetic stirrer hot plate set temperature at 37 °C and magnetic stir bar was used in achieving homogeneous temperature to prevent solidification of the mixture solution. 300 μ L 3% agarose gel solution was first filled in a 10mm × 10mm plastic mold, 3 to 4 spheroids were then collected in 5 μ L spheroids suspension and mixed with 100 μ L 3% agarose gel solution followed by immediately dispensed in the center of the mold. The mold was placed flat on ice to allow the agarose to cool until it's entirely solidify, the solidified agarose was then cropped with an 8-mm diameter tube. This procedure created a 4-mm thickness agarose phantom in 8 mm diameter with micrometastases spheroids suspended in the center of the phantom.

2.3 Paired-agent staining and rinsing protocol

To test the feasibility of the ratiometric pairedagent imaging method to estimate the binding potential of cancer cells, 8-mm diameter lymph node biological model was developed considering the size of human lymph node. MDA-MB-231 tumor spheroids with 250 µm in diameter were encapsulated in lymph node phantom to mimic the clinical condition of micrometastatic lymph nodes. A targeted and control imaging solution was used to evaluate the diffusion of both imaging agent in the lymph node phantom in the presence of cancer cells. ABY-029, a clinically relevant anti-EGFR affibody, was labeled with a nearinfrared fluorophore, IRDye-800CW (LICOR Bioscience) as targeted imaging agent and hydrolyzed IRDye-700DX (LICOR Bioscience) was used as control agent.

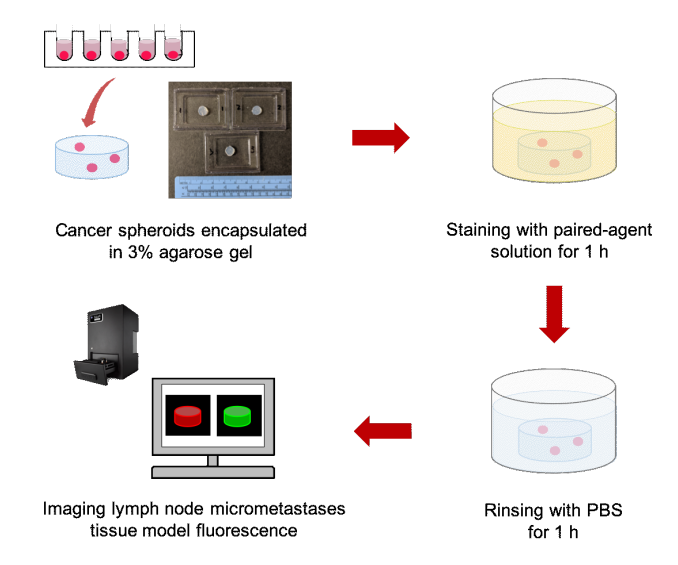


Figure 1. Stepwise illustration of lymph node micrometastases model staining and rinsing procedure.

Lymph node micrometastases tissue model was created according to the protocol mentioned in 2.2. A pre-staining image was acquired to evaluate background levels caused by autofluorescence. A mixture of targeted and control imaging agent for each node was prepared at concentration of 0.1 μM IRDye800-ABY029 and 0.2 μM hydrolyzed IRDye700DX. Lymph nodes were soaking in the paired-agent staining solution that covered with an aluminum foil to protect it from light at room temperature. After 1 hour of staining, the lymph node was submerged in phosphate-buffered saline (PBS) for rinsing with light protection at room temperature. Whole lymph node tissue phantom was immediately imaged under an 85-μm resolution fluorescence imaging system (Pearl Imager, LICOR Biosciences). Fluorescence at 700-740 nm and 800-840 nm (from 685 and 785 nm excitation, respectively) were acquired to evaluate diffusion and binding of both targeted and control imaging agents after the staining and rinsing process. Autofluorescence was removed by subtracting the pre-staining image of respective imaging channels from subsequent post-staining-and-rinsing images. The signal intensity of the targeted and control imaging agents were compared to evaluate their concentration of intact lymph node phantom.

Fluorescence images of lymph node phantoms(n=3) was used to evaluate distribution of control and targeted imaging agents. **Fig 2a** displays the lymph node phantoms uptake of control imaging agent (hydrolyzed IRDye700DX, shown in red) and the uptake of targeted imaging agent (IRDye800CW labeled ABY-029 affibody, shown in green), respectively. These figures demonstrated that with the staining and rinsing process, both imaging agents are capable of penetrating the entire lymph node phantom. And the distribution for the control and targeted agents are nearly identical in the locations that did not contain cancer spheroids. Only in cancerous locations was the retention of the targeted agent significantly higher than the control agent. Binding potentials were then calculated as mentioned above on a pixel-by-pixel basis shown in **Fig 2a**. **Fig 2b** demonstrated that the binding potential of targeted agent was found to be 0.652 ± 0.130 in the presence of binding of the mircometastases regions, which was statistically significantly higher than the binding potential measured at the non-cancerous regions of -0.008 ± 0.042 (p < 0.0001). These results highlight the unprecedented potential of using paired-agent imaging with this staining and rinsing protocol to significantly improve the sensitivity of cancer detection of clinically important micrometastases in excised lymph nodes.

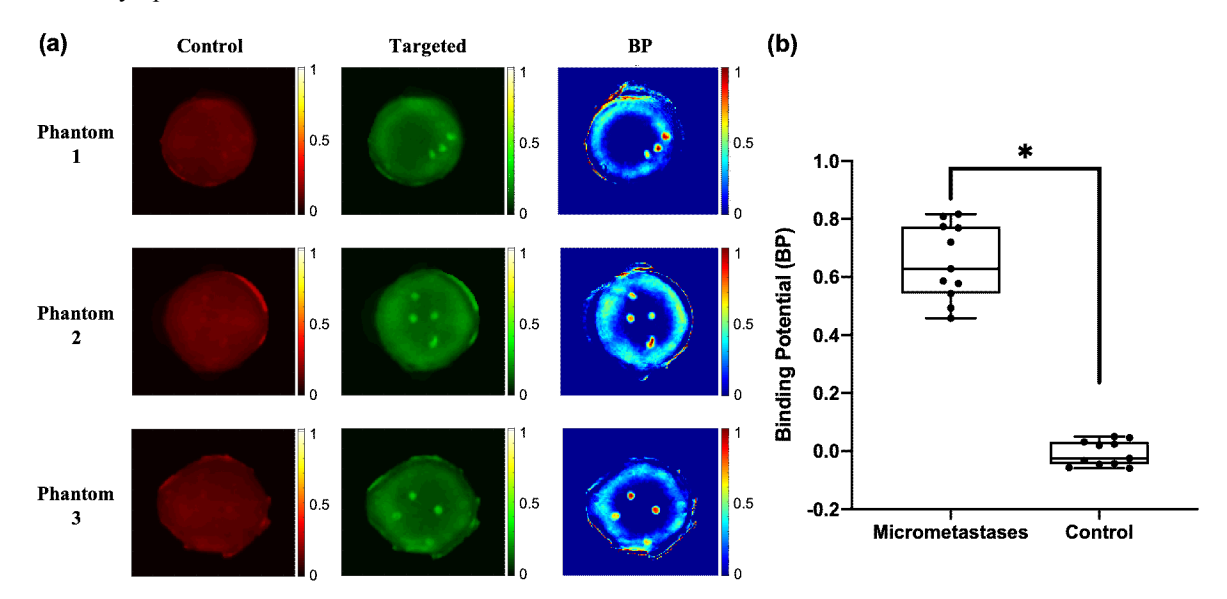


Figure 2. Paired-agent staining and rinsing protocol in lymph node micrometastases phantom.

3. CONCLUSIONS

With distribution of both imaging agents achieved in the entire lymph node after prolonged staining and rinsing, the results demonstrate the potential of ex vivo paired-agent staining and imaging of whole human lymph nodes. The

results demonstrated the advantage of this paired-agent imaging ratiometric approach, which will be implemented into our image reconstruction using angular restriction optical tomography projection. With 250-µm diameter cancer cells spheroid "micrometastases" model implants into a lymph node, the paired-agent fluorescence imaging and gold standard fluorescence protein microscopy would be compared to evaluate the ability to significantly improve the sensitivity of cancer cells detection for sentinel lymph node biopsy.

ACKNOWLEDGMENTS

The authors acknowledge support from the NSF CAREER 1653627, the Nayar Prize at IIT, and the Department of Biomedical Engineering at the Illinois Institute of Technology.

REFERENCES

- [1] S. L. Chen, D. M. Iddings, R. P. Scheri *et al.*, "Lymphatic mapping and sentinel node analysis: current concepts and applications," CA Cancer J Clin, 56(5), 292-309; quiz 316-7 (2006).
- [2] M. A. Swartz, and M. Skobe, "Lymphatic function, lymphangiogenesis, and cancer metastasis," Microsc Res Tech, 55(2), 92-9 (2001).
- [3] G. H. Lyman, A. E. Giuliano, M. R. Somerfield *et al.*, "American Society of Clinical Oncology guideline recommendations for sentinel lymph node biopsy in early-stage breast cancer," J Clin Oncol, 23(30), 7703-20 (2005).
- [4] D. L. Weaver, "Pathology evaluation of sentinel lymph nodes in breast cancer: protocol recommendations and rationale," Mod Pathol, 23 Suppl 2, S26-32 (2010).
- [5] E. J. Wilkinson, L. L. Hause, R. G. Hoffman *et al.*, "Occult axillary lymph node metastases in invasive breast carcinoma: characteristics of the primary tumor and significance of the metastases," Pathol Annu, 17 Pt 2, 67-91 (1982).
- [6] N. Apostolikas, C. Petraki, and N. J. Agnantis, "The reliability of histologically negative axillary lymph nodes in breast cancer. Preliminary report," Pathol Res Pract, 184(1), 35-8 (1988).
- [7] K. Tew, L. Irwig, A. Matthews *et al.*, "Meta-analysis of sentinel node imprint cytology in breast cancer," Br J Surg, 92(9), 1068-80 (2005).
- [8] M. Trojani, I. de Mascarel, J. M. Coindre *et al.*, "Micrometastases to axillary lymph nodes from invasive lobular carcinoma of breast: detection by immunohistochemistry and prognostic significance," Br J Cancer, 56(6), 838-9 (1987).
- [9] "Prognostic importance of occult axillary lymph node micrometastases from breast cancers. International (Ludwig) Breast Cancer Study Group," Lancet, 335(8705), 1565-8 (1990).
- [10] P. J. Hainsworth, J. J. Tjandra, R. G. Stillwell *et al.*, "Detection and significance of occult metastases in node-negative breast cancer," Br J Surg, 80(4), 459-63 (1993).
- [11] S. Friedman, F. Bertin, H. Mouriesse *et al.*, "Importance of tumor cells in axillary node sinus margins ('clandestine' metastases) discovered by serial sectioning in operable breast carcinoma," Acta Oncol, 27(5), 483-7 (1988).
- [12] P. Ambrosch, and U. Brinck, "Detection of nodal micrometastases in head and neck cancer by serial sectioning and immunostaining," Oncology (Williston Park), 10(8), 1221-6; discussion 1226, 1229 (1996).
- [13] R. J. Cote, H. F. Peterson, B. Chaiwun *et al.*, "Role of immunohistochemical detection of lymph-node metastases in management of breast cancer. International Breast Cancer Study Group," Lancet, 354(9182), 896-900 (1999).
- [14] K. M. Tichauer, K. S. Samkoe, J. R. Gunn *et al.*, "Microscopic lymph node tumor burden quantified by macroscopic dual-tracer molecular imaging," Nat Med, 20(11), 1348-53 (2014).

- [15] L. Sinha, F. Massanes, V. C. Torres *et al.*, "Comparison of time- and angular-domain scatter rejection in mesoscopic optical projection tomography: a simulation study," Biomed Opt Express, 10(2), 747-760 (2019).
- [16] V. C. Torres, C. Li, Y. He *et al.*, "Angular restriction fluorescence optical projection tomography to localize micrometastases in lymph nodes," J Biomed Opt, 24(11), 1-4 (2019).
- [17] M. A. Mintun, M. E. Raichle, M. R. Kilbourn *et al.*, "A quantitative model for the in vivo assessment of drug binding sites with positron emission tomography," Ann Neurol, 15(3), 217-27 (1984).
- [18] K. M. Tichauer, Y. Wang, B. W. Pogue *et al.*, "Quantitative in vivo cell-surface receptor imaging in oncology: kinetic modeling and paired-agent principles from nuclear medicine and optical imaging," Phys Med Biol, 60(14), R239-69 (2015).
- [19] K. M. Tichauer, K. S. Samkoe, W. S. Klubben *et al.*, "Advantages of a dual-tracer model over reference tissue models for binding potential measurement in tumors," Phys Med Biol, 57(20), 6647-59 (2012).
- [20] C. Li, V. C. Torres, and K. M. Tichauer, "Noninvasive detection of cancer spread to lymph nodes: A review of molecular imaging principles and protocols," J Surg Oncol, 118(2), 301-314 (2018).
- [21] C. Li, X. Xu, N. McMahon *et al.*, "Paired-Agent Fluorescence Molecular Imaging of Sentinel Lymph Nodes Using Indocyanine Green as a Control Agent for Antibody-Based Targeted Agents," Contrast Media & Molecular Imaging, 2019, 13 (2019).
- [22] M. Zanoni, F. Piccinini, C. Arienti *et al.*, "3D tumor spheroid models for in vitro therapeutic screening: a systematic approach to enhance the biological relevance of data obtained," Sci Rep, 6, 19103 (2016).
- [23] S. Sant, and P. A. Johnston, "The production of 3D tumor spheroids for cancer drug discovery," Drug Discov Today Technol, 23, 27-36 (2017).
- [24] R. C. Bates, N. S. Edwards, and J. D. Yates, "Spheroids and cell survival," Crit Rev Oncol Hematol, 36(2-3), 61-74 (2000).
- [25] Y. J. He, D. A. Young, M. Mededovic *et al.*, "Protease-Sensitive Hydrogel Biomaterials with Tunable Modulus and Adhesion Ligand Gradients for 3D Vascular Sprouting," Biomacromolecules, 19(11), 4168-4181 (2018).
- [26] Y. J. He, M. F. Santana, M. Moucka *et al.*, "Immobilized RGD concentration and proteolytic degradation synergistically enhance vascular sprouting within hydrogel scaffolds of varying modulus," J Biomater Sci Polym Ed, 1-26 (2019).